Simplified model of a novel direct-drive PTO based on an azimuthal linear switched reluctance generator

Marcos Blanco, Miguel Santos-Herrán, Gustavo Navarro, Jorge Torres, Jorge Najera, Luis García-Tabares, Marcos Lafoz

Abstract— **One of the key challenges in wave energy conversion is the improvement of the Power Take-Off (PTO) system. The paper is based on a novel linear switched reluctance generator (LSRG) to be used as PTO. This new azimuthal topology of a LSRG improves the force density and reduces the use of magnetic material - hence, reducing its cost. This new LSRG has been analysed in detail, optimising the control parameters and evaluating the efficiency, power, and force maps. A detailed PTO model is used, which includes a detailed electric machine model, a power electronics converter model and low-level control algorithms. This paper presents a methodology for using these maps to define a simplified PTO model version. This simplified model is a PTO-loss model which provides the electric power from the instantaneous velocity and force. A comparison between the results obtained with the simplified and detailed PTO models is performed, in terms of accuracy and computational load. From this analysis, the PTO-loss model is considered adequate to be used in Wave to Wire models due to its low computational cost. The presented methodology will be applied to the development of the azimuthal LSRG to derive its simplified model from real data obtained by characterisation tests. However, it can be used in a broader way to obtain simplified models of any PTO from either detailed models or real data.**

Keywords*— *Wave Energy, Power take-off, Point Absorber, Loss model.

I. INTRODUCTION

IN marine energy, a *Power Take-Off* (PTO) is defined as the "mechanism that converts the motion of the prime mover into a useful form of energy such as electricity", and *prime mover* is defined as the "marine energy converter (MEC) component that interfaces with a resource from which energy is converted"[1]. In our particular case study, the MEC is a floating buoy which interacts with the waves, and the PTO is a linear electric generator which brakes the buoy movement and generates electricity.

The PTO is, therefore, a key component in wave energy conversion in charge of generation of electric energy [2]. As a consequence, a good understanding of the PTO behaviour, this is, a good PTO modelling, is essential to evaluate the performance of a MEC. The main reasons for this can be further detailed as: 1) the losses of the PTO must be considered and quantified in order to evaluate the final "useful form of energy" generated, and 2) the energy extraction algorithms must integrate the PTO performance and rated characteristics (i.e. maximum displacement) in the form of either efficiency or losses [3]–[7].

The energy extraction algorithm defines the force to be developed by the PTO in order to extract energy from the waves. The force command can be split in 2 terms (see Fig. 1): 1) active force: which is in phase with the velocity, and 2) reactive force: which lags velocity 90º and has a null average value. The aim of the application of reactive force is the achievement of mechanical resonance in the MEC, maximizing the mechanical generated power [8], [9]. However, the use of the reactive force implies electrical losses while not generating net electric energy. In consequence, the objective function of the maximization should be the electric energy and the energy extraction algorithm would evaluate this variable by means of a PTO model.

The PTO loss model proposed can be used both, in the evaluation of the electric energy of a MEC (in particular in Wave Energy Converters – WEC) and it can be integrated in energy extraction control (e.g. in Model Predictive Controls [9], [10]). The model has been parametrized for the azimuthal linear switched reluctance generator that is being developed at SEATITAN project [11]–[14]. It is worth mentioning that this kind of PTO (direct-drive linear electric generator) generates an oscillating electric power which should be smoothed prior to be injected in the grid. The proposed loss model could be useful in the design of power smoothing systems such as energy storage systems both integrated in WECs and connected to

Paper ID: 2061, EWTEC2021, Grid integration, power take-off and control.

This research, developed under the Project SETITAN (ID: 764014), has received funding from European Union's Horizon 2020 research and innovation programme under H2020-EU.3.3.2. - Low-cost, lowcarbon energy supply (LCE-07-2016-2017).

M. Blanco, M. Santos-Herrán, G. Navarro, J. Torres, J. Najera, L. García-Tabares, and M. Lafoz are with CIEMAT, Av. Complutense 22, 28040 Madrid, Spain (e-mails: marcos.blanco@ciemat.es, Miguel.santos@ciemat.es, jorgejesus.torres@ciemat.es, Jorge.najera@ciemat.es, gustavo.navarro@ciemat.es, luis.garcia@ciemat.es, marcos.lafoz@ciemat.es).

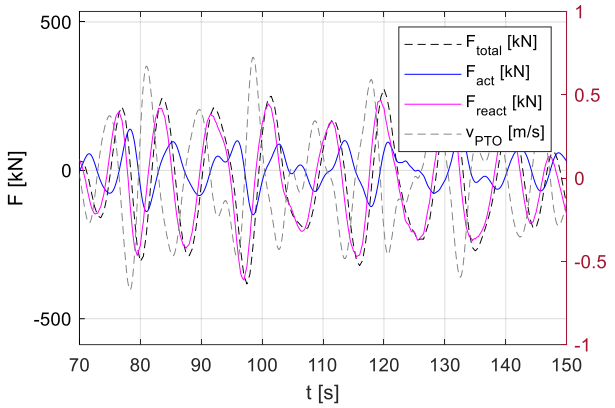

Fig. 1. Velocity and force (split into its active and reactive components) in the PTO.

the onshore PCC (point of common coupling) of a wave farm [15], [16].

II. BASIC CONCEPTS OF THE PROPOSED PTO MODEL

In order to evaluate the PTO losses, a loss model is proposed. This model can assess the losses in the PTO (including both linear generator and power electronics) but ignores the dynamic behaviour of the electric variables of the PTO. The main implication is that the current command is considered instantaneously imposed and hence, the force command. The mechanical variables of the PTO would be simulated integrated in a WEC model in a standard way

The inputs for this model are the mechanical variables which interconnect it to the broader global WEC model. The outputs are the generated electrical power, the efficiency and the power losses. The total losses to be considered (P_{loss}) are (see (1)):

- Mechanical losses (P_{L_mec}): e.g., losses in the linear bearings and guides of the PTO. These losses are mainly dependent on the velocity of the system, so, in this case, these are neglected due to the low velocity displacement values of wave energy systems. In a similar PTO configuration (linear electric SRM machine of 200kW) the losses in lab test in vertical position reach a maximum value of approx. 1% of the nominal power [17].
- Magnetic losses (P_{L_mag}): Foucault losses and hysteresis losses. These losses are dependent on the current frequency, so, in this case, these are also neglected because of the low current frequency in the linear generator (again related the low system velocities).
- Power electronic losses (P_{L_PE}): conduction and switching losses. They depend on the current value and frequency, respectively. These losses are also neglected in a first approach due to the high efficiency of this type of device.
- Electric losses (P_{L_el}): Joule power losses in the wires and coils of the PTO. These losses are dependent on the current in the linear generator. Joule losses have a great impact on the total PTO losses since, for the same target power, low velocities lead to high force values, which require high current values in the linear generator.

$$P_{loss} = P_{L\_mec} + P_{L\_mag} + P_{L\_PE} + P_{L\_el} \cong P_{L\_el} \quad (1)$$

The electric power generated by the device (P_{el}) can then be obtained by subtracting the total losses from the absorbed mechanical power (P_{mec}):

$$P_{el} = P_{mec} - P_{loss} = P_{mec} - P_{L-el} = \cdots \\ \ldots = F_{pto} \cdot v_{pto} - P_{L-el} \quad (2)$$

Therefore, electric power production can be evaluated ultimately from mechanical variables (force and velocity), which, in turn, are the inputs to the PTO loss model. Only the electric losses still need to be expressed in terms of mechanical variables. Since electric losses are the square of the current multiplied by the electric resistance of the generator coils (R_{pto}), and, in the case of (linear) electric machines, current (I_{pto}) is approximately proportional to force (F_{pto}), this gives:

$$P_{L-el} = R_{pto} \cdot (I_{pto})^2 = \ldots \\ \ldots = R_{pto} \cdot (K_{F-I} \cdot F_{pto})^2 = R'_{pto} \cdot (F_{pto})^2 \quad (3)$$

where, for the machine considered in the present study:

$$R'_{pto} = R_{pto} \cdot (K_{F-I})^2 = R_{pto} \cdot \left(\frac{I_{pto-nom}}{F_{pto-nom}}\right)^2 = \cdots \\ \ldots = 0.1192[\Omega] \left(\frac{350[A]}{35[kN]}\right)^2 = 11.92 \cdot 10^{-6} \left[\frac{s}{kg}\right] \quad (4)$$

The equation (4) uses a linear simplification of the relationship current-force. In addition, in switched reluctance machines, it is known that:

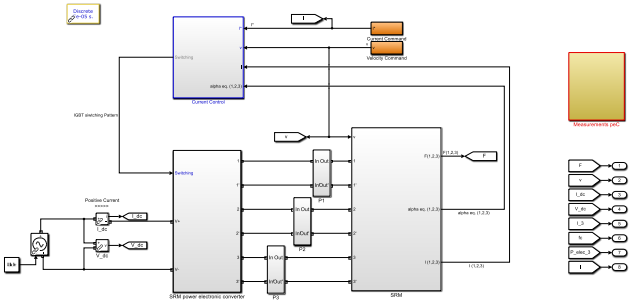

Fig. 3. Simulink scheme of the detailed PTO model.

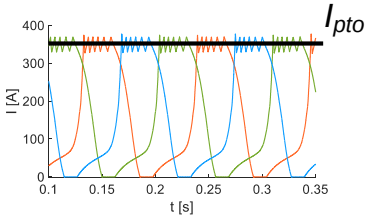

I_{pto} : current command
$i_a(t)$, $i_b(t)$, $i_c(t)$: instantaneous phase current

Fig. 2. Electric current time profiles in the generator's coils evaluated with the detailed PTO model.

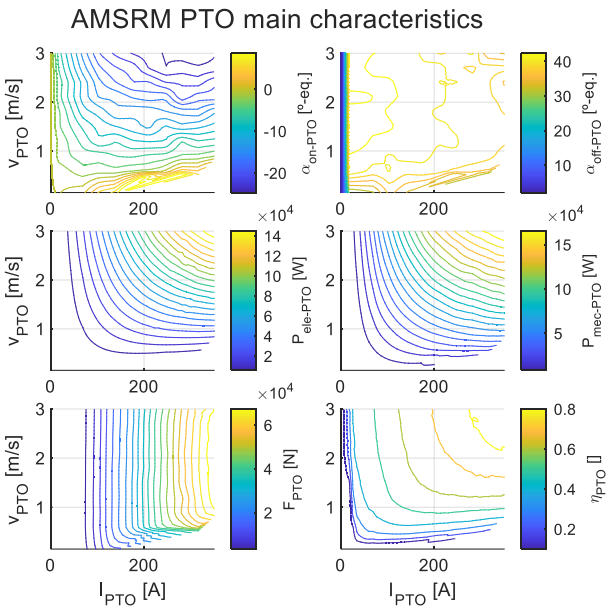

Fig. 5. AMSRM PTO main characteristics, with respect to velocity and current: *(top left)* activation angle; *(top right)* deactivation angle; *(middle left)* electric power; *(middle right)* mechanical power; *(bottom left)* PTO force; *(bottom right)* PTO efficiency.

$$I_{pto} \sim \begin{cases} k \cdot {F_{pto}}^2, & at\ low\ current\ values \\ k \cdot F_{pto}, & for\ the\ rest\ of\ the\ values \end{cases} \quad (5)$$

The magnetic circuit of the electric machine is not-saturated at low currents and hence the magnetic field is proportional to the current. Considering that the force is the product of the magnetic field by the current, the force is proportional to the squared current. However, at high currents, the magnetic field can be considered almost constant, and this fact leads to a linear relationship between force and current [18].

So, it would be possible to express losses as $P_{L-el} = R_{pto} \cdot {I_{pto}}^2(F_{pto})$ where $I_{pto}(F_{pto})$ is a piecewise function as defined in (5). Equation (5) improves the accuracy with respect to (4) due to the inaccuracy which introduces the neglecting of the quadratic relationship of current and force at low current values. This piecewise function (5) is parametrized and its results are presented in the section V.

III. DETAILED PTO ELECTRIC MODEL

A. Description

A detailed PTO electric model has been implemented in MATLAB-Simulink (see Fig. 2), including the following features:

- A dynamic model of the linear generator based on data obtained from FEM analysis;
- A power electronics model (taking into consideration commutation switches);
- A discrete current control algorithm which controls the states of the diverse power electronics switches. The current control implemented is a soft-switching hysteresis band control [18].

It is worth mentioning that the current command is used as an input to the PTO loss model (I_{pto}). This value is used as a representative average value of the phase currents in the linear generator (see Fig. 3).

The detailed electric PTO model allows to:

- Simulate the electromagnetic behaviour of the complete PTO (linear generator + power electronics).
- Parametrise and optimise the current control values. In particular, a differential evolutionary algorithm [19] has been utilised to obtain the phase activation/deactivation position that maximise the energy extraction (see first two subplots in Fig. 4) as described in [13]. The phase activation/deactivation positions are evaluated offline, and the optimum value for each current and velocity value is applied by means a look-up table.
- Once the optimum control parameters have been applied, evaluate the performance of the PTO, in terms of force, power and efficiency (see subplots 3 to 6 in Fig. 4)

B. Detailed model vs loss model

As presented above, in order to assess the PTO losses, either the PTO loss model or the detailed PTO electric model might be employed. The former is able to compute losses, but does not incorporate the electric dynamic behaviour, whereas the latter can simulate the electromagnetic behaviour.

WEC models usually consider simulations of operation times ranging from dozens of minutes to hours, and utilise

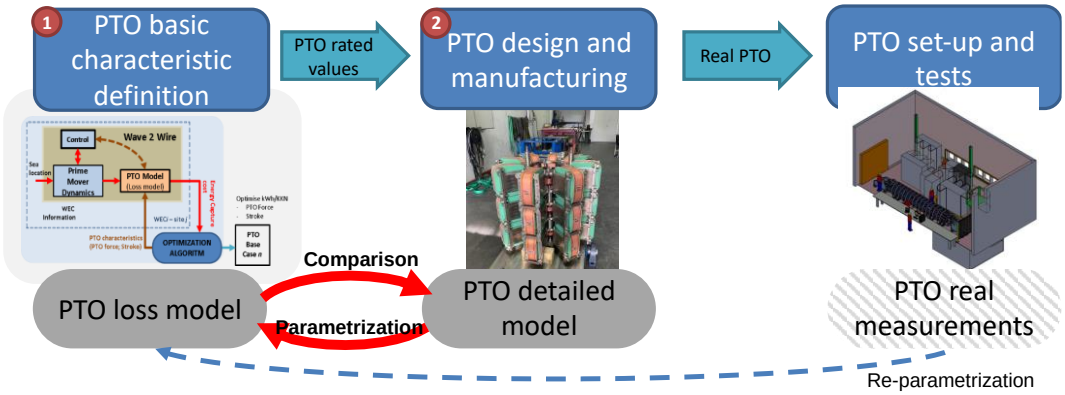

Fig. 4. Project stages in the development of SEA-TITAN's PTO.

sampling times adapted to the aforementioned periods (for example, hundreds of milliseconds). In practice, the force command in a PTO can be computed by the control system in hundreds of microseconds, and a specific force command (starting from a null value) can be imposed in milliseconds. As a consequence, the PTO dynamics and transient evolutions might be neglected when comparing with the WEC dynamics. A second consequence is that the implementation of a detailed PTO electric model (with sampling times of microseconds) into a WEC model leads to excessive computational efforts.

On the contrary, the PTO loss model can be evaluated at the same sampling time as the WEC model. Hence, the PTO loss model is more suitable when used in combination with WEC models.

IV. THE PTO LOSS MODEL IN THE SEA-TITAN PROJECT

Under the H2020 SEA-TITAN project, a novel PTO has been developed. The PTO comprises an electric linear generator (based on a switched reluctance machine), the power electronics and the associated control system. Both the PTO loss model and the detailed PTO electric model have been utilised in the design of this PTO.

The project has been organised as follows (see Fig. 5):

1) The basic PTO characteristics have been defined. At this stage, the PTO rated values have been calculated so as to meet the requirements of some specific WEC designs and deployment locations. At this stage, the PTO loss model has been used.
2) The PTO has been designed in detailed and manufactured. At this point, the detailed PTO electric model was employed.
3) The manufactured PTO is set up, commissioned and tested in a laboratory.

The PTO loss model is initially parametrised with the nominal/rated values from stage 1, but these parameters are re-computed by integrating the results of the detailed PTO electric model from stage 2 and the measured values from stage 3 with the real PTO.

Finally, this re-parametrised PTO loss model is validated against the results obtained from the detailed model in new scenarios different from the ones used for the parametrisation. This parametrisation and validation are explained in the following section.

The study case considered in this paper is for a PTO designed for a 2-body WEC, based on WEDGE GLOBAL technology [20], in BiMEP location [21]. According to the pre-dimensioning tool described in [22], the rated characteristics of the PTO are 105 kN and 3 m/s composed of 3 modules of LSRG of 35 kN. These rated characteristics have been used in subsection V.B, however, the parametrization of the model has been carried out with 2 LSRG modules (70 kN) due to the way to implement the electric detailed model. The rated current of the PTO module is 350A, and the rated voltage of the PTO module of the DC link is 450V.

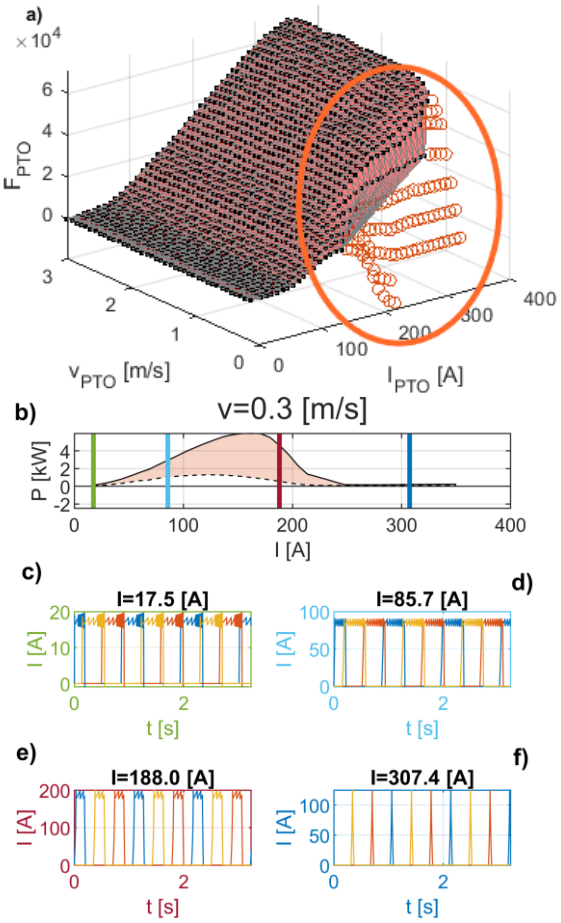

Fig. 6. *(a)* Surface of force values with respect to current command and velocity; *(b)* Power generation with respect to current at low velocity (0.3 m/s); *(c-f)* Activation/deactivation times at low velocity (0.3 m/s) for different values of current.

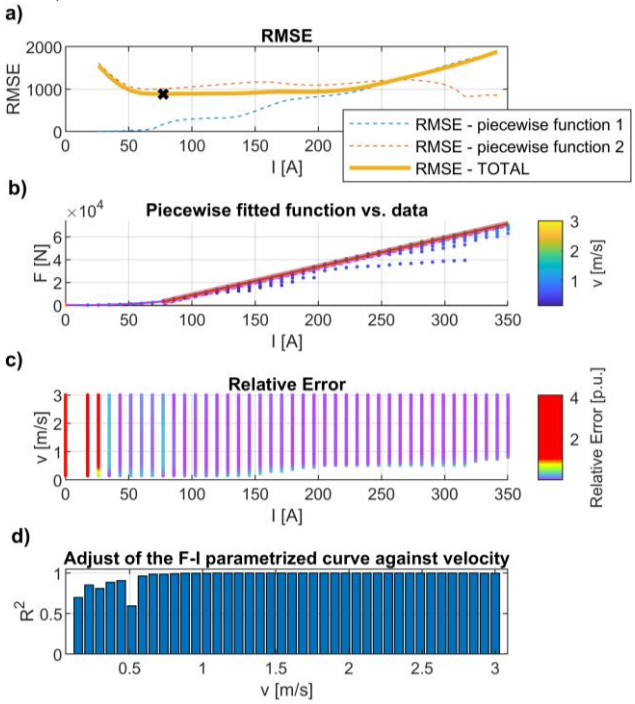

Fig. 7. *(a)* Root Mean Square Error (RMSE) for the piecewise function with respect to current; *(b)* Comparison of the force piecewise function fit vs simulation data; *(c)* Relative error in force with respect to current and velocity; *(d)* Statistical "coefficient of determination" R^2 values of the fit with respect to velocity.

TABLE I
PARAMETER VALUES FOR THE PIECEWISE CHARACTERISATION OF F_{PTO}

PIECEWISE FUNCTION	Parameter	Value
F_{pto}^{inf}	k_{11}	165.5
	k_{12}	-21.83
	k_{13}	0.8246
F_{pto}^{sup}	k_{21}	$-1.63 \cdot 10^4$
	k_{22}	250.5
	I_{lim}	77.1795

V. PARAMETRIZATION OF POWER TAKE-OFF LOSS MODEL

A. PTO loss model parametrisation

In order to parametrise the PTO loss model, the results from the detailed PTO electric model are employed. More specifically, the results utilized are obtained from scenarios with constant current command and velocity.

1) Current-Force relationship parametrization

The first step in the model parametrisation is the characterisation of the force-current-velocity relationship. The results from the detailed PTO electric model are shown in the form of a $F_{pto}(I_{pto}, v_{pto})$ surface in Fig. 6-a. Some relevant conclusions can be drawn from it, such as:

- Strong dependence of force on current. The theoretical relationship between force and current outlined in (5) is observed: linear dependence at high current values and quadratic dependence at low current values.
- The influence of velocity on force is negligible; only relevant in low-velocity high-current scenarios.
- The current command (I_{pto}). is used as representative value of the average current in the linear generator.
- The outlier values (see circled area in Fig. 6-left) are discarded.

The rationale for the last point above is the following: at low velocities, force increases with current for low current values. However, at a certain current value a maximum force is reached and then force starts to decrease with current. The reason for this is that at those conditions (I_{pto}, v_{pto}), the generated power is low (due to the low velocity) but losses are high (due to Joule losses linked to the high current). The activation/deactivation angles are optimised to maximise the electric power, so, in those conditions, they tend to reduce the activation time (see Fig. 6-b) of the phases to minimise the Joule losses and avoid negative generated power values (i.e., to avoid consuming electricity instead of generating it). It can be observed then that, in those conditions, for a given velocity v_{pto}, there will be two different values for current giving the same resulting force. The lower current value is selected and the upper one is considered 'outlier' and is discarded.

As a consequence of all the aforementioned observations, the relationship force-current-velocity $F_{pto}(I_{pto}, v_{pto})$ is then represented as a piecewise function where the influence of velocity has been neglected:

$$\begin{aligned} I_{pto} < I_{lim} &\rightarrow F_{pto}^{inf} = k_{11} + k_{12} \cdot I_{pto} + k_{13} \cdot {I_{pto}}^2 \\ I_{pto} \geq I_{lim} &\rightarrow F_{pto}^{sup} = k_{21} + k_{22} \cdot I_{pto} \end{aligned} \quad (6)$$

The piecewise function is shown in (6), and uses a quadratic expression at low current values and a linear function at high current values. The current threshold is determined by I_{lim}. The values for the parameters in (6) are shown in Table I. Such values have been adjusted to minimise the error between the piecewise function fit and the actual data, as shown in the first two subplots in Fig. 7. A Least-Squares Fitting method has been used to fit the equation [23].

The relative error and the quality of the fit worsen at low current and velocity values (see the last two subplots in Fig. 7). The last subplot in Fig. 7 supports the decision of neglecting the influence of the velocity for most of its range of values (0.6 to 3 m/s). However, at low velocities (<0.6 m/s). its effect becomes important.

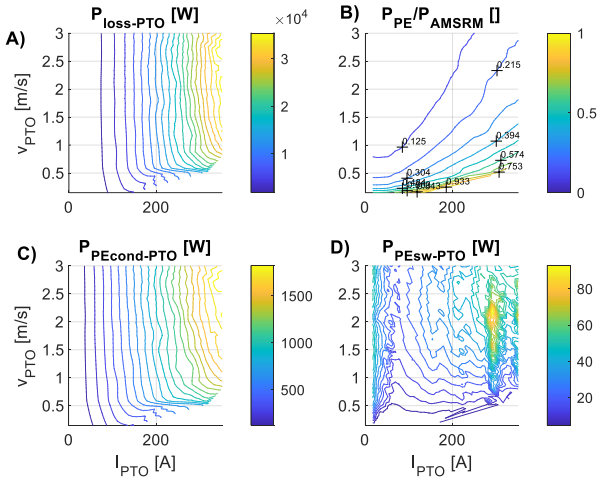

Fig. 8. PTO power losses evaluated at constant current and velocity. A. Joule power losses; B. Power electronic conduction power losses; C. Power electronic switching power losses; D, Ratio between Joule loses and total power electronic losses.

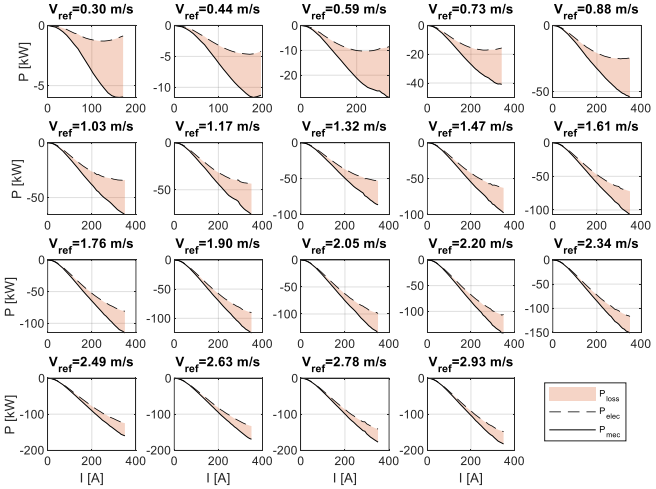

Fig. 9. PTO generated mechanical power (P_{mec}), electric power (P_{elec}) and power losses (P_{loss}) evaluated at constant current and velocity.

TABLE II
FORCE-LOSSES RELATIONSHIP PARAMETERS

PIECEWISE FUNCTION	Parameter	Value
P_{loss}^{sup}	q_{23}	4.609e-06
	q_{22}	0.1494
	q_{21}	1616
P_{loss}^{inf}	q_{12}	0.6795
	q_{11}	37.42
	F_{LIM}	77.1795

TABLE IV
SEA CLIMATE SCENARIOS USED IN W2W SIMULATIONS

Case	H_s [m]	T_p [s]	Extracted mechanical power [W]
1	1.5	6.0	4479.1
2	2.0	7.5	4705.8
3	3.0	9.0	5058.7
4	4.0	11.0	6005.6
5	5.0	13.0	6008.2
6	1.0	6.0	3270
7	1.5	8.0	3795.8
8	2.5	8.0	6396.7
9	2.0	10.0	3100.3
10	4.5	10.0	6855.7
11	3.0	12.0	3040.3
12	4.0	14.0	4578

TABLE III
SEA CLIMATE SCENARIOS USED W2W SIMULATIONS

Case	Power losses (detailed model) P_{loss1} [W]	Power losses (loss model) P_{loss2} [W]	Relative error $(P_{L2}- P_{L1})/P_{L1}$
1	3364.4	3582.7	6.49%
2	3454.7	3699.1	7.08%
3	3765	4105.4	9.04%
4	4046.5	4331.8	7.05%
5	4000.8	4187.1	4.66%
6	2848.7	3041	6.75%
7	3218.4	3498.4	8.70%
8	4228.1	4444.8	5.13%
9	2913.7	3192.6	9.57%
10	4462.8	4707.1	5.47%
11	2810.8	3063.6	8.99%
12	3368.8	3522.3	4.56%

2) Power Losses-Force relationship parametrization

As a second step in the development of the loss model, the relationship between the force developed by the linear electric generator F_{pto} and the power losses P_{loss} is parametrised.

In a first analysis, results obtained from the detailed model simulations at constant velocity v_{PTO} and current I_{pto} (see Fig. 8) are studied. The figure shows that: 1) as total losses P_{loss} are driven by Joule losses P_{L_el}, they present a quadratic relationship with current and with force (the latter, at high values of the current); 2) there is a strong dependence of losses on current but a slight dependence on velocity (except for low-velocity high-current scenarios); 3) power electronic losses P_{L_PE} are negligible compared with the total losses. In addition, Fig. 9 plots the power profiles with respect to the linear electric generator current for each constant velocity, showing that losses are relatively small at high current and velocity values. However, at low velocities, the electric power could be even negative (consumption instead of generation). This operation mode is called, in electric machines, "non-regenerative brake" and implies that power losses P_{loss} are higher than the energy generated, implying a negative resulting final power (consumption).

As described in section II, the relation (force)-(power losses) has been implemented as a piecewise function where the influence of the velocity has been neglected. Taking into account the theoretical considerations about the relationship between force and current, and keeping in mind that power losses are driven by Joule losses [4]; the following behaviour are observed: a quadratic relationship between force and losses at low force values and a linear behaviour at high force values.

The piecewise function is represented in (7), and the values of its parameters are shown in Table I.

$$\begin{aligned} F_{pto} < F_{lim} &\rightarrow P_{loss}^{inf} = q_{11} + q_{12} \cdot F_{pto} \\ F_{pto} \geq F_{lim} &\rightarrow P_{loss}^{sup} = q_{21} + q_{22} \cdot F_{pto} + q_{23} \cdot {F_{pto}}^2 \end{aligned} \quad (7)$$

The force function fit of the above equation to the original data computed with the PTO detailed model is shown in Fig. 10. The proposed piecewise equation has been fitted to the simulation data by means of a Least-Square Fitting method [23] and its coefficients are shown in Table II.

A. Comparison between loss model and detailed model

In the previous sub-section, the PTO loss model has been parametrised by using the results of the PTO detailed model from simulations at different constant velocities and current commands. The parametrised loss model has been compared to the results of the PTO detailed model in long-term scenario simulations (400 s). Table III shows the 12 simulated scenarios, which are representative of the sea location of the case study (BIMEP [24]) and considered a 2-body WEC simulated by means of a wave-to-wire (W2W) model [22].

The electric power profiles obtained from the detailed model and the loss model for the 12 cases are shown in Fig. 11. Table IV shows the results of the mean electric power and power losses obtained by both models. In addition, the comparison of the evaluation of losses by each model is also presented.

Results show in all cases an error below 10%, which allows to consider the usage of the loss model at MEC design stages where simulations cover periods from dozens of minutes to hours by using sampling times of hundreds of milliseconds.

The comparison in computation time required depending on the chosen type of model is as follows: an average time of 1 hour and 45 minutes per case when using the detailed model vs an average time of 30 seconds per case when using the loss model (i9-7920X/128GB RAM).

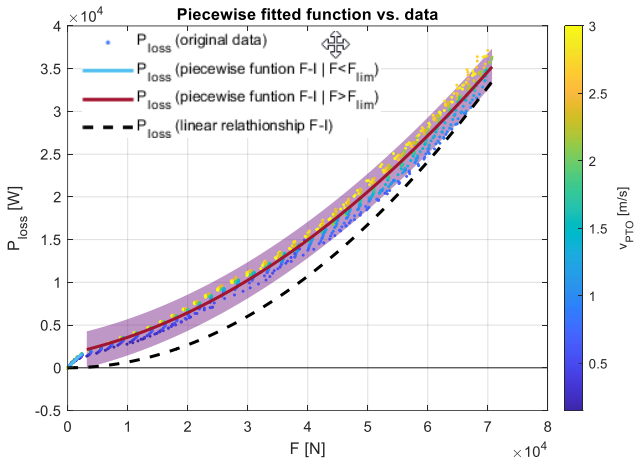

Fig. 12. PTO loss model fit (relationship force-losses). Original data and loss model results.

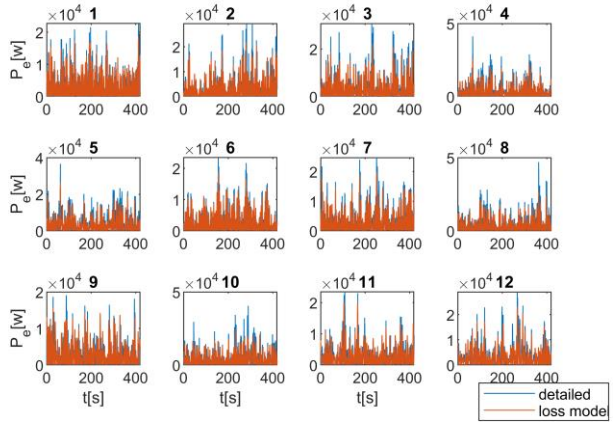

Fig. 10. Generated electric power profiles for the 12 simulated cases with a PTO detailed model (blue) and with a PTO loss model (red).

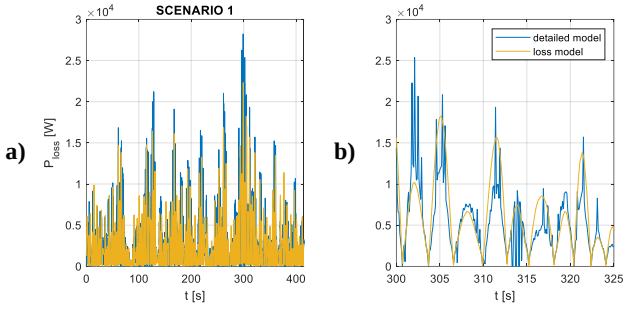

Fig. 11. Detail of the electric losses power profiles of scenario 1 evaluated with the detailed model and PTO loss model. *a)* complete simulation; *b)* zoomed-in detail of a 25-second section.

In addition, it is also worth mentioning that the reduced PTO loss model provides results with a mean error of the 12 simulation cases under the 7% for average or mean values (as shown in Table IV). Fig. 12 shows an example of the matching in the results from the point of view of the dynamic behaviour. The reason for the differences observed could be that the detailed model incorporates the commutation of power electronics, which leads to some "ripple" over the power losses profile, while the profile obtained from the loss model is smoother (Fig. 12.b).

VI. CONCLUSION

Building upon the advantages of the inclusion of a PTO model in WEC models, this work describes a PTO model based on the evaluation of the losses that are present in a direct-drive PTO (in particular, linear electric generator). The utilisation of a PTO model allows to evaluate the electric production of a WEC and should be integrated in the control algorithm to calculate the mechanical commands in order to maximise the final electric power instead of the intermediate mechanical power.

At certain design stages, the implementation of a simpler PTO loss model preferable to an electric detailed model due to the reduction in computational time of simulations (a 200-fold reduction in computational effort of the simulation can be reached).

The results of this reduced PTO loss model have been reviewed and compared with an electric detailed model in long-term scenarios with acceptable results: error under 10% and a good matching of the time profile behaviours.

In this work, the PTO loss model has been parametrised from the electric detailed model data, but in the coming future it will be parametrised from the real data obtained in the lab tests over an electric linear generator by applying the same methodology. First, a series of tests will be carried out at constant velocity and force to parametrise the model, followed by emulation of the WEC behaviour in order to validate the parametrisation.

ACKNOWLEDGEMENT

The authors thanks to: WAVEC Offshore Renewables (and in particular to Miguel Vicente) for the collaboration in the development of the Wave2Wire model; WEDGE GLOBAL S.L. for the sea climate and WEC data.

REFERENCES

[1] "IEC TS 62600-1:2020 | Marine energy - Wave, tidal and other water current converters - Part 1: Vocabulary." ISO, p. 17, 2020, Accessed: Apr. 16, 2021. [Online]. Available: https://webstore.iec.ch/publication/64583.

[2] J. L. Villate, "Strategic Research and Innovation Agenda for Ocean Energy," 2020. [Online]. Available: https://www.etipocean.eu/news/targeted-innovation-to-drive-large-scale-deployment-of-ocean-energy-says-new-etip-ocean-report/.

[3] M. Blanco *et al.*, "Meta-heuristic optimisation approach for wave energy converter design by means of a stochastic hydrodynamic model," *IET Renew. Power Gener.*, p. rpg2.12021, Jan. 2021, doi: 10.1049/rpg2.12021.

[4] D.-E. Montoya Andrade, A. de la Villa Jaén, and A. García Santana, "Considering linear generator copper losses on model predictive control for a point absorber wave energy converter," *Energy Convers. Manag.*, vol. 78, pp. 173–183, Feb. 2014, doi: 10.1016/j.enconman.2013.10.037.

[5] E. Tedeschi and M. Molinas, "Tunable Control Strategy for Wave Energy Converters With Limited Power Takeoff Rating," *IEEE Trans. Ind. Electron.*, vol. 59, no. 10, pp. 3838–3846, 2012, doi: 10.1109/TIE.2011.2181131.

[6] P. Garcia-Rosa, G. Bacelli, and J. Ringwood, "Control-Informed Geometric Optimization of Wave Energy Converters: The Impact of Device Motion and Force Constraints," *Energies*, vol. 8, no. 12, pp. 13672–13687, Dec. 2015, doi: 10.3390/en81212386.

[7] G. Bacelli and J. V Ringwood, "A geometric tool for the analysis of position and force constraints in wave energy converters," *Ocean Eng.*, vol. 65, pp. 10–18, 2013, doi: http://dx.doi.org/10.1016/j.oceaneng.2013.03.011.

[8] J. Falnes, *Ocean Waves and Oscillating Systems, Linear Interactions Including Wave-Energy Extraction*. Cambridge: Cambridge University Press, 2002.

[9] J. Hals, J. Falnes, and T. Moan, "A Comparison of Selected Strategies for Adaptive Control of Wave Energy Converters," *J. Offshore Mech. Arct. Eng.*, vol. 133, p. 31101, 2011, doi: 10.1115/1.4002735.

[10] A. de la Villa Jaén, A. García-Santana, and D. El Montoya-Andrade, "Maximizing output power of linear generators for wave energy conversion," *Int. Trans. Electr. Energy Syst.*, vol. 24, no. 6, pp. 875–890, Jun. 2014, doi: 10.1002/etep.1747.

[11] European Union, "Commission Regulation (Eu) 2016/631," *Off. J. Eur. Union*, no. 14 April 2016, p. 68, 2016.

[12] L. Garcia-Tabares Rodriguez *et al.*, "New Type of Linear Switched Reluctance Generator for Wave Energy Applications," *IEEE Trans. Appl. Supercond.*, p. 1, 2020, doi: 10.1109/TASC.2020.2981900.

[13] M. Blanco, G. Navarro, and M. Lafoz, "Control of power electronics driving a switched reluctance linear generator in wave energy applications," in *Power Electronics and Applications, 2009. EPE '09. 13th European Conference on*, 2009, pp. 1–9.

[14] M. BLANCO AGUADO *et al.*, "SWITCHED RELUCTANCE MACHINE," ES2728442A1, 2019.

[15] I. Villalba *et al.*, "Wave farms grid code compliance in isolated small power systems," *IET Renew. Power Gener.*, vol. 13, no. 1, pp. 171–179, Oct. 2019, doi: 10.1049/iet-rpg.2018.5351.

[16] T. Kovaltchouk, A. Blavette, J. Aubry, H. Ben Ahmed, and B. Multon, "Comparison Between Centralized and Decentralized Storage Energy Management for Direct Wave Energy Converter Farm," *IEEE Trans. Energy Convers.*, vol. 31, no. 3, pp. 1051–1058, Sep. 2016, doi: 10.1109/TEC.2016.2547462.

[17] M. Santos *et al.*, "Testing of a full-scale PTO based on a Switched Reluctance Linear Generator for Wave Energy Conversion," 2012, [Online]. Available: https://www.icoe-conference.com/publication/testing_of_a_full_scale_pto_based_on_a_switched_reluctance_linear_generator_for_wave_energy_conversion/.

[18] T. J. E. Miller, *Switched Reluctance Motors and Their Control (Monographs in Electrical and Electronic Engineering)*. Clarendon Press, 1993.

[19] R. Storn, "System design by constraint adaptation and differential evolution," *Evol. Comput. IEEE Trans.*, vol. 3, pp. 22–34, 1999, doi: 10.1109/4235.752918.

[20] http://wedgeglobal.com/, "WEDGE Global S.L. Homepage," 2015. http://wedgeglobal.com/ (accessed Jun. 14, 2015).

[21] "Bimep - Área de ensayos de energía marina de Armintza." http://bimep.com/ (accessed Oct. 12, 2015).

[22] M. Blanco *et al.*, "Implementation of an energy extraction control including PTO-losses in a complete WEC model for PTO design procedure," 2019.

[23] D. Borowiak, "Linear Models, Least Squares and Alternatives," *Technometrics*, vol. 43, no. 1, p. 99, 2001, doi: 10.1198/tech.2001.s549.

[24] BiMEP, "Mutriku Technical Characteristics – BiMEP." https://www.bimep.com/en/mutriku-area/technical-characteristics/ (accessed Jan. 15, 2021).